Empirical Noise Modeling of Internally Mixed Exhaust Systems

JAMES BRIDGES[†]
NASA Glenn Research Center, 21000 Brook Park Rd, Cleveland, OH 44135

There appear to be no non-proprietary methods to predict the noise of internally mixed exhaust systems, and no guidance for how to adapt known jet noise models for these configurations. This paper surveys literature and historical databases acquired at NASA Glenn's Aero-Acoustic Propulsion Lab to give such guidance. The core premise is that an exhaust system with well-designed mixer produces noise that is to first approximation the same as a fully-mixed jet flow. Refinement of what is meant by a "fully mixed jet" can lead to more accurate prediction of the main jet noise. Additional noise is often generated within the nozzle, typically at high frequencies, whose source mechanism(s) are not obvious. However, a noise prediction method can be established that captures some aspects of the excess noise and provide an estimate of the total jet noise. Explorations of source mechanisms associated with the internal mixer have led to a new noise model which includes the effects of having an external plug nozzle, a feature desirable for near-term supersonic aircraft. Statistical analysis of historical data is provided to estimate the uncertainty in using this method given the variations found that cannot be directly computed without detailed mixer geometry.

I.

II. Nomenclature

U	fully expanded velocity
De	area-equivalent nozzle diameter
T	temperature
BPR	bypass ratio
NPR	nozzle total pressure ratio, P_t/P_∞
NTR	nozzle total temperature ratio, T_t/T_∞
M	gas Mach number, U/a
Ma	acoustic Mach number, U/a_∞
a	speed of sound
PSD	power spectral density
P	sound power
l_p	external plug length
l_m	mixer length
h_m	mixer lobe height, peak to peak
dx	distance, mixer exit to nozzle exit
ϕ	polar angle
f	frequency
k	flight exponent in flight correction

Subscripts

b	bypass
c	core
mix	mixed
1S	single-stream
2S	dual-stream
XS	excess component
t	total (stagnation)
∞	ambient, external to exhaust system

[†] Acoustics Branch, M/S 54-3; AIAA Associate Fellow

III. Motivation

NASA has a long-standing effort to reduce barriers to a commercial supersonic transport market. One barrier is the noise produced by aircraft during landing and take-off (LTO) operations. First principles indicate that aircraft with high supersonic cruise performance will produce more LTO noise than conventional aircraft. Careful engineering will be required to balance LTO noise with cruise performance, and it is critical that noise predictions be accurate. When doing conceptual design for such aircraft empirical noise prediction methods need to be quick and require few detailed variables. The tools used in such studies should produce noise estimates plus an uncertainty which reflects the range of results that might come from a well-designed nozzle. Such prediction methods need not include details on how to optimize the nozzle. The method will not reflect how loud a poorly designed nozzle might be, but should reflect best practices as they are known today. Luckily, in the case of internally mixed exhaust systems the geometric characteristics of a good aero design are not in conflict with a quiet design.

Internally mixed exhaust systems are primarily of interest for lower bypass ratio propulsion systems where nacelle weight and drag is not a driving factor. The additional propulsive efficiency of the internal mixing (up to 4%) is worth the extra hardware and wetted surface. In the 1990's as typical bypass ratios for commercial airliners went above 5 these types of nozzles seem to have lost favor. From NASA aero studies [1,2] it appears that the thrust performance difference between an optimized mixer and a basic design is relatively small, $O(0.1\%)$. Perhaps this is why not much research has been published on mixer design as factors such as weight, manufacturability, and maintenance are more critical for a successful overall design. Additionally, while several papers documented work done in the era of early turbofan engines, none of the commonly available empirical noise prediction methods claim to predict the noise of these configurations [3–7].

The historical literature does contain anecdotal information about unexpected noise sources encountered in experiments [8–10]. The source of the extra noise was debated, but rarely definitively identified. Perhaps the most detailed work on such a noise source is in [11,12]. Design practices within manufacturers is rarely debated as new designs are not common. However, the renewed interest in propulsion systems for commercial supersonic aircraft has awakened the need for better understanding of parasitic noise sources and potential noise reduction approaches for these systems.

In any aeroacoustic application there are often multiple mechanisms to create sound. While the basic jet plume has a very robust and predictable noise spectral directivity, there are many opportunities in the high-speed ducting of an exhaust system to create new noise sources: cavities that whistle, blunt shapes with wakes, points of unsteady separation, etc. [13]. Any unsteady flow phenomena can become a significant noise problem if it has enough kinetic energy and can efficiently couple with the acoustic wave field. Internally mixed exhaust systems have a high proclivity for creating additional noise sources in that they contain two shear layers, which are amplifiers of perturbations, and a closed duct which supports acoustic coupling. This is especially true when the inner mixer is an axisymmetric splitter, the simple symmetry providing support for direct feedback between the two shear layers [14]. Other amplifiers can exist in the system if there are unsteady separations or shocks within the nozzle. This coupled system can and has produced resonances which result in noise characterized as subtle broadband amplification through to highly phased-locked tones. Part of the problem with empirically modeling the noise of these systems is accounting for the subtle ways in which such resonances can occur.

The bulk of this paper will be taken up with proposing an empirical modeling approach that is less ambitious in its scope than some reported efforts, not requiring CFD input for example [12]. It assumes that the user is looking for high-level estimates of jet noise and that acoustically poor designs will be removed at a later stage in development. Most importantly, this work hopes to provide an uncertainty estimate to bound the range of noise that could be produced by realistic lobed mixer designs.

IV. Noise Database

In-house work creating a design system for lobed mixers and using this for aero optimization studies has given the impression that there are a wide array of mixer designs that can produce good aero performance [1,2]. The lack of detailed acoustic prediction tools precludes a similar optimization of mixer design for acoustic performance. While the creation of such a tool is still needed for preliminary design work after the basic parameters of the exhaust system have been established, we are left with the use of historical databases of mixer designs that were created for a mix of aero and acoustic reasons, some more enlightened than others. In this paper the mixer designs were basic, having lobes that were all identical on a given mixer.

To produce an empirical noise model for internal mixers we reached back to several test campaigns conducted at NASA Glenn's Aero-Acoustic Propulsion Lab (AAPL). The work has been published in various details in prior papers [6,7,15]. All models were designed by aero industry engineers, some as model-scale versions of company products, and tested at flow conditions reflecting realistic engine cycles. Most were tested at several flight speeds, including none (static). More recently, an exhaust system designed by NASA was tested in which a single mixer was evaluated with variations in the nozzle length and external plugs of different lengths [16–18]. Far-field acoustic spectra were acquired in a similar fashion for all these nozzle systems, making the database self-consistent. The combined dataset of 251 test points were used to create an empirical noise prediction method and to statistically quantify the errors from the method, as discussed in this paper.

In this work we'll not describe the five nozzles of different lengths, the nine mixers, and plug geometries of the exhaust systems in the database being used to create or noise model. Nor will we list all the flow conditions; only flow parameters needed for the modeling will be shown. Some of the data contains proprietary engine geometry and cycle information, but all represent turbofan engines designed in the 1990-2000 time frame. Geometries range from axisymmetric splitters to scalloped lobed mixers. Model-scale nozzle diameters range from 120mm to 185mm. Flows can be described by fully mixed acoustic Mach numbers Ma_{mix}, total temperature ratios NTR_{mix}, fully mixed velocity ratios U_b/U_c, and flight speed M_∞. Geometrically, the mixers are parameterized by lobe divergence angle, defined by peak-to-peak lobe height relative to lobe length (h_m/l_m). In the case of geometries with external plugs, the plug will be characterized by its length relative to the equivalent nozzle diameter (l_p/D_e). These entities are visually defined in Figure 1Other parameters were considered in creating the models, but were discarded as not having unique impact on the noise. Figure 2 shows the range of the parameters in the database. Different color symbols represent distinctly different mixer designs and are kept consistent in this report.

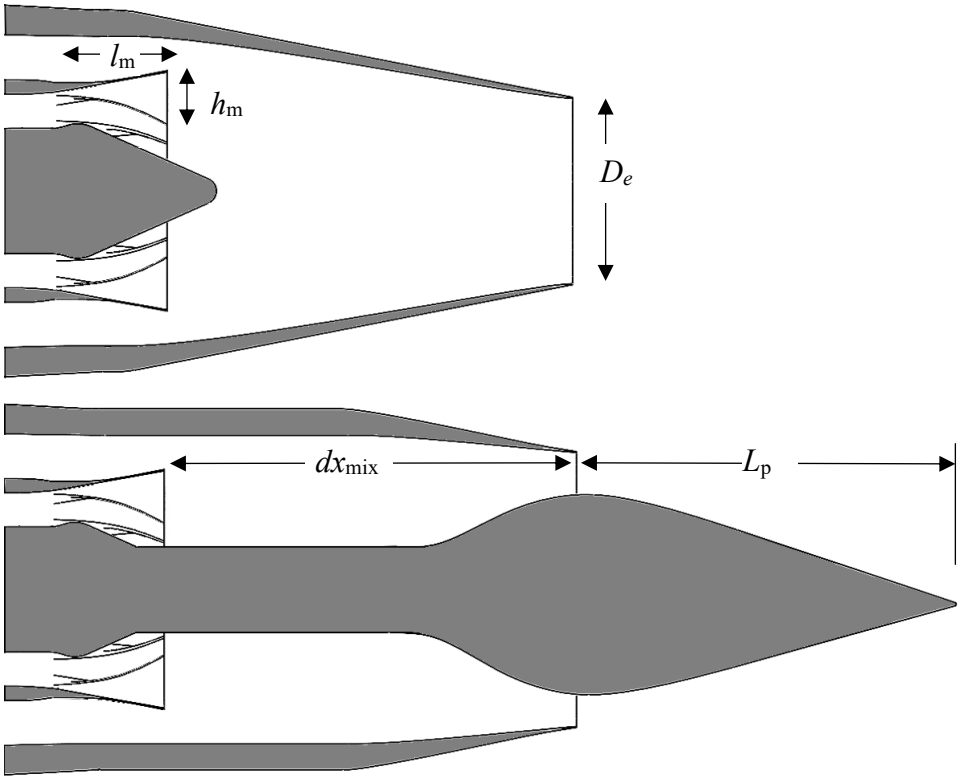

Figure 1 Exhaust system geometry definitions

Data has been transformed into power spectral density (*PSD*) of the acoustic pressure for ease of scaling and analysis. In most plots the data is presented as *PSD*, model-scale, rescaled to an arc with an arbitrary 2-nozzle diameter radius, with atmospheric attenuation restored. Much of the database was acquired with the nozzles operating in a flight environment provided by an open freejet. The corrections used to transform the experimental data to an infinite wind tunnel with the observer moving with the nozzle are given in [19]. In all cases the source was assumed to be at the nozzle exit and due to the size of the freejet and large distance to the microphones (> 60D) the impact of this assumption is less than 1dB for subcritical jet flows.

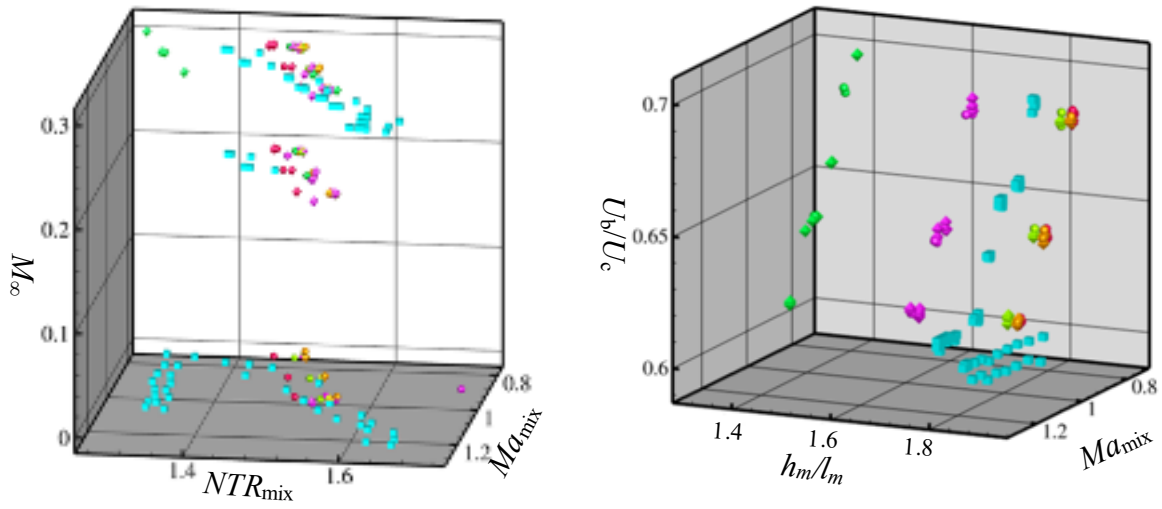

Figure 2 Parameter space of database used in model development.

V. Development of method

In the following section we will develop a model for the spectral directivity of the noise of a two-stream jet with fully mixed core and bypass velocities, total temperatures, and flight stream M_∞. This model for the noise of a two-stream jet, denoted PSD_{2S}, will be based on the idea that if the mixer were perfect and didn't create any additional noise then the noise would be that of a single-stream jet, denoted as PSD_{1S}, that has the velocity and temperature of the fully mixed fluid. Any additional noise produced by the mixing is called 'excess noise', PSD_{XS}.

$$\boldsymbol{PSD_{2S}(f,\emptyset) = PSD_{1S}(f,\emptyset) + PSD_{XS}(f,\emptyset)} \qquad \text{Eq. 1}$$

where f is frequency, ϕ is polar angle, measured from the direction of flight. Importantly, the two terms on the right-hand side are in sound power, not dB, *i.e.* they come from independent sources.

We start with an engine's exhaust demands in terms of pressure and temperature of the gases provided to the mixer. This is often produced by a one-dimensional engine analysis along with mass flows of the two streams and is often the information given to the acoustician making their noise estimate. From this, one knows the fully expanded velocities of the two streams. Depending upon the ratio of the pressures of the two streams and the geometry of the duct and mixer, the actual nozzle pressure ratio of the combined streams can be known but this often requires CFD as the complex duct interactions require consideration of duct geometries. To simplify the analysis we use the independent, fully expanded core and bypass velocities (U_c, U_b) and bypass ratio (BPR) to compute a mass-averaged ideally expanded and fully mixed jet velocity:

$$U_{mix} = (U_c/(1+BPR) + U_b/(1/BPR+1))$$

The fully mixed total temperature $T_{t,mix}$ is similarly calculated substituting T_t of the two streams for their velocities. To make the analysis independent of ambient temperature, we normalize the fully mixed jet velocity by ambient speed of sound a_∞ and temperature T_∞ and work with acoustic Mach number Ma_{mix} and nozzle total temperature ratio NTR_{mix}:

$$Ma_{mix} = U_{mix}/a_\infty$$
$$NTR_{mix} = T_{t,mix}/T_\infty$$

These two quantities, along with the nozzle diameter, are used as inputs to a single-stream jet noise prediction method. This would be the first approximation for PSD_{1S}. In this work we are using the NASA code *'sjet' [20]*, which is similar to the code described in [21]. The primary benefit over older codes is that these methods predict noise in power spectral density making their data easier to transform. Obviously the quality of this single-stream noise code is critical, but that isn't the point of the current work.

For flows with a non-zero ambient flight speed U_∞, a flight correction has to be applied to the predicted results (*sjet* only predicts noise of static jets). Our approach is the same as commonly used (see [22]), but uses a flight exponent approach that uses an exponent $k(f,\phi)$ that is dependent upon both frequency and polar angle. Examples can be found in [16,17]. The basic form of the adjustment to the *PSD* of a static jet with jet velocity U_{mix} when $U_\infty \neq 0$ is

$$\frac{PSD_{\text{flight}}(f,\phi)}{PSD_{\text{static}}(f,\phi)} = \left(\frac{U_{mix}-U_\infty}{U_{mix}}\right)^{k(f,\emptyset)} \qquad \text{Eq. 2}$$

The result of using Ma_{mix}, NTR_{mix}, and flight speed M_∞ can be seen in Figure 3 which compares the prediction with experimental data for an exhaust system used in [18]. The flow has matched pressures on the core and bypass ($NPR_c = NPR_b = 1.8$), with $NTR_c = 3.2$ and $NTR_b = 1.2$, and $M_\infty = 0.3$. The colors on the shape of the spectral directivity denote the difference between prediction and data as a function of frequency and polar angle, measured from the upstream axis. By the color bar we see that for most frequencies and angles the *PSD* of the simple single-jet prediction is below that of the data by several dB.

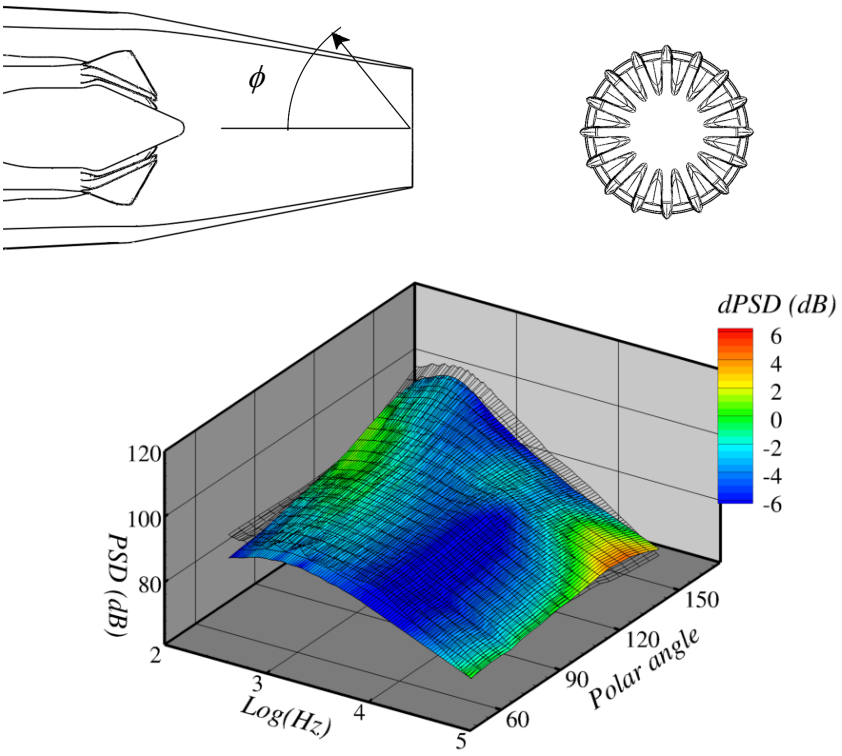

Figure 3 Spectral directivity of internally mixed nozzle with lobed mixer, experiment and single-stream prediction using Ma_{mix}. Surface shape is *PSD* of prediction; color shows difference between prediction – data, in dB.

This same calculation is done for all the cases in our noise database using the prediction code *sjet* and the simple fully mixed Ma_{mix}. For a more quantified analysis, we start by looking at the low-frequency portion of the spectral directivity, specifically frequencies below $St = 0.5$ based on U_{mix}. We look at data over this range because when model-scale data is transformed to full-scale and flown in the manner of aircraft certification, two distinct regions emerge as being important for the certification metric Effective Perceived Noise Level (EPNL): low frequencies below $St = 0.5$ at aft angles around 130°, and high frequencies where humans are most responsive to noise (~2kHz) and where the aircraft is closest to the observer (~95°). For some systems with loud fan noise the higher frequency noise may not be critical to overall EPNL. For systems with dominant jet noise, such as are expected for supersonic air travel, it is critical that both regions of the spectral directivity be accurately predicted. For internally mixed exhaust systems there is typically a clear dividing point in frequency above which the differences due to the mixer have a strong impact. For the cases in our database this line was consistently near $St = fD/U_{\text{mix}} = 1$. The 'excess noise' of the mixer designs is usually found in the frequencies above this line. The lower frequencies are more dominated by the parameters of the equivalent fully mixed jet plume.

For simple jets, the lower frequencies are dominated by the aft peak, and their directivity is predicted well. Therefore, to quantify the external, fully mixed jet noise we simply integrate the spectral directivity over the polar angles to obtain the band-limited overall sound power levels (OAPWL) for frequencies below $St = 0.5$. Comparison of this metric from data and from prediction give a good measure how well the key low-frequency aft portion of the noise is predicted. We will call this quantity P_{1S} to indicate that it is the sound power of the single-stream approximation to the jet noise *PSD*:

$$P_{1S} = \int_{St=0}^{0.5} \int_{\emptyset} PSD(f, \emptyset) d\emptyset dSt$$

Figure 4 shows a plot of P_{1S} from experimental data of various exhaust systems and engine cycle points projected onto the parameters Ma_{mix} and NTR_{mix}. Note that for a given Ma_{mix} there are several points at different flight velocities adding to the spread of the data. The point of standard single-stream jet noise prediction, such as *sjet*, is to collapse these data onto a single plane.

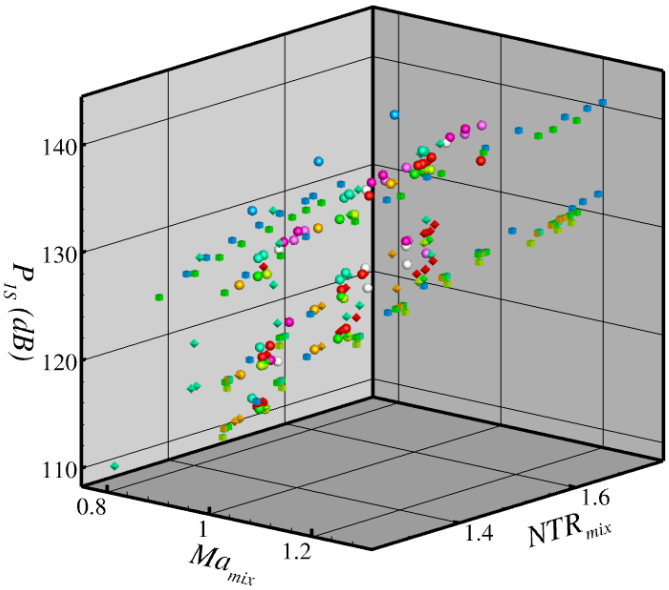

Figure 4 Scatter plot of P_{1S} from data as a function of mixed acoustic Mach number Ma_{mix} and NTR_{mix} for all cases in database. Colors indicate different exhaust system geometries.

Figure 5 shows the difference ΔP_{1S} between P_{1S} from the *sjet* prediction and P_{1S} from the data. With the gross effect of jet and flight velocity removed the difference appears relatively random over the flow parameter space (Ma_{mix}, NTR_{mix}), and reflects the error in this first-order approximation. Quantitatively, the average of ΔP_{1S} is -1.35dB with a standard deviation of 1.58dB.

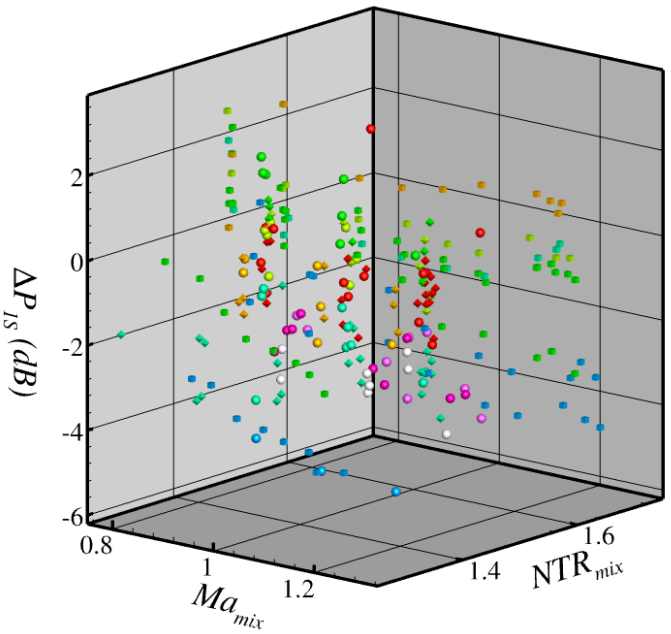

Figure 5 Scatter plot of ΔP_{1S} as a function of mixed acoustic Mach number Ma_{mix} and NTR_{mix} for all cases in database. Colors indicate different exhaust system geometries.

When one plots ΔP_{1S} as a function of mixer parameters, such as mixer lobe divergence h_m/l_m, and velocity ratio U_b/U_c, a pattern emerges (Figure 6). Mixers with less penetration and lower velocity ratio generally produce more low frequency noise than ones with high penetration and high velocity ratio. This seems reasonable. Velocity ratios closer to 1 would mean less mixing is

required to get to a fully mixed state with lower high-speed streaks exiting the nozzle. Higher penetration would, to first order, correlate with better mixing and less chance of a high speed streak being left at the nozzle exit to energize the plume turbulence.

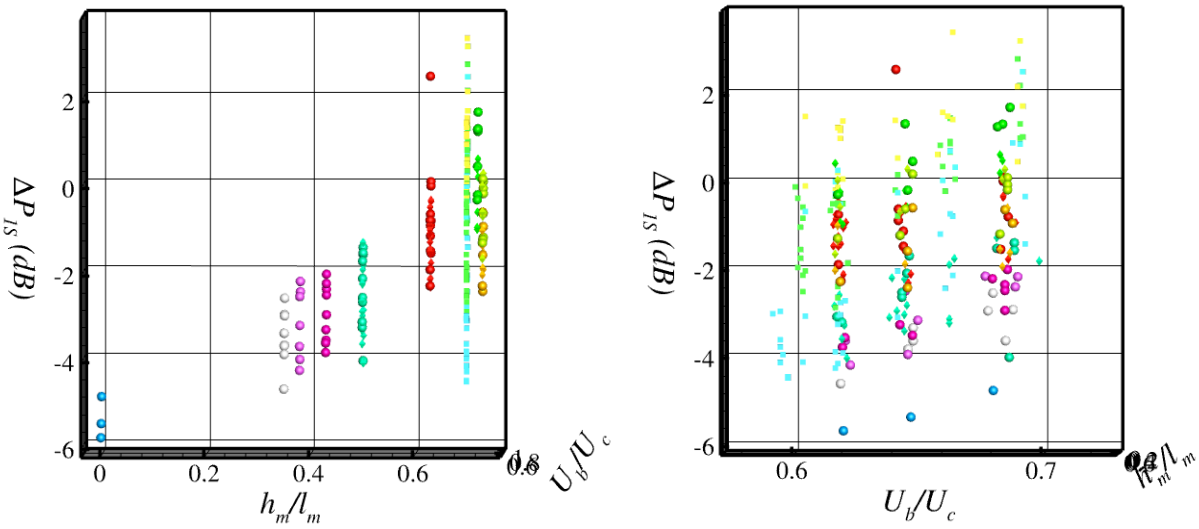

Figure 6 Scatter plot of ΔP_{1S} as a function of mixer lobe divergence h_m/l_m and velocity ratio U_b/U_c for all cases in database. Colors indicate different exhaust system geometries.

This leads to a corrective model for the single-stream, fully mixed approximation. We could simply expect that less internal mixing amplifies the external jet mixing noise and make a model for an additive term (in dB) to be applied to the *sjet* result. But we have chosen to make the correction apply to the fully mixed velocity used in the basic single-stream jet noise prediction. This choice emphasizes how the impact of having unmixed high-speed streaks in the flow is to effectively increase the velocity of the jet plume. The values of ΔP_{1S} are translated into a model for a modified mixed velocity, Ma_{mix}*, based on velocity ratio and mixer lobe height, equating the impact of the mixer to the physics of jet mixing sources. Assuming an $80log_{10}(Ma_{mix}*/Ma_{mix})$-dependence at all polar angles for a small change in Ma_{mix}, we replot the data in Figure 6 in terms of a Mach-correction factor $Ma_{mix}*/ Ma_{mix}$, creating Figure 7, and show a simple model to fit the data.

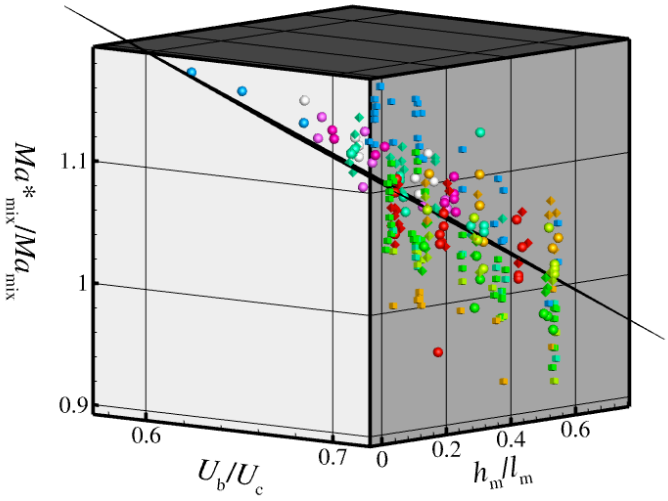

Figure 7 Scatter plot of P_{1S}, recast as ratio of fully mixed acoustic Mach number, as a function of mixer lobe height and velocity ratio for all cases in database. Mesh surface is model for Ma_{mix}* (Eq. 3). Colors indicate different exhaust system geometries.

The strong impact of velocity ratio over the mid-range typical of turbofan engines ($0.55 < U_b/U_c < 0.7$) makes it difficult to create a simple function that meets this and still has $Ma_{mix}*/Ma_{mix}$ go to 1 as U_b/U_c goes to 1. Lacking data between $0.7<U_b/U_c<1$, a piecewise function capturing the strong behavior in the mid-range and linearly tapering to 1 as U_b/U_c goes to 1 should be adopted. It is unlikely that many propulsion systems would fall outside the mid-range of velocity ratio. The final model for the modified mixed velocity, $Ma_{mix}*$ is

$$Ma^*_{mix} = \frac{Ma_{mix}}{\left(1-(0.66(1-U_b/U_c)-0.15(h_m/l_m)-0.075)\right)}, \quad U_b/U_c < 0.7. \qquad \text{Eq. 3}$$

Predictions of *PSD* are now made with *sjet* using $Ma_{mix}*$ (NTR_{mix} is not changed); these are denoted $PSD_{1S}*$ and the extracted low-frequency sound power is $P_{1S}*$. The differences between the predicted $P_{1S}*$and experimental P_{1S} are much smaller: the average of the low frequency $\Delta P_{1S}*$ is -0.26dB with a standard deviation of 1.04dB. Visually, this is shown in Figure 8 where the scatter is greatly reduced compared to Figure 6.

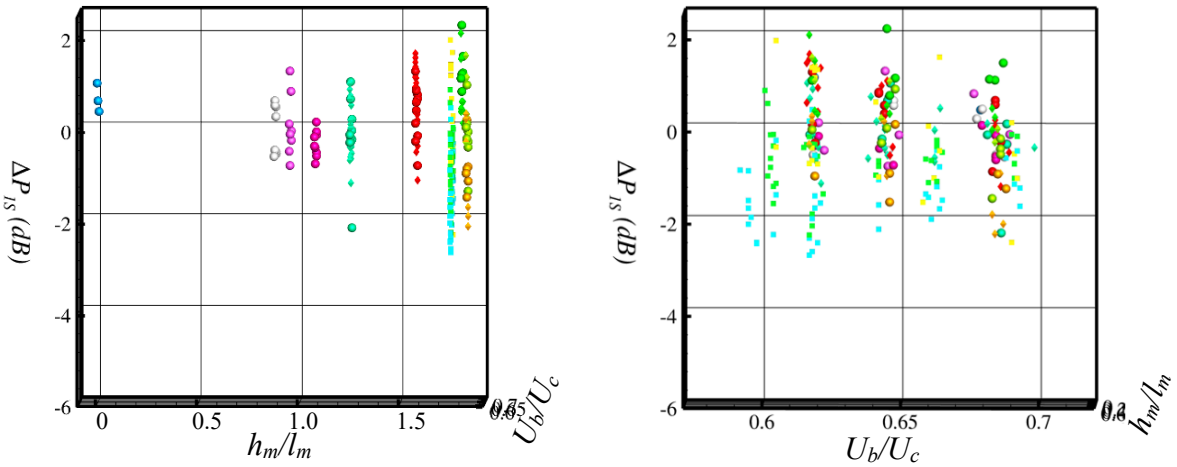

Figure 8 Scatter plot of $\Delta P_{1S}*$ as a function of mixer lobe height and velocity ratio for all cases in database.

When we plot the predicted $PSD(f,\phi)$ of the example case against the data, such as done in Figure 9, the discrepancy between prediction and data, *dPSD,* is visually closer to zero (more green!). The prediction of the low frequencies is certainly much better than with the original value of Ma_{mix}.

So now our model for the PSD of the two-stream exhaust system has been modified slightly from Equation 1:

$$\boldsymbol{PSD_{2S}(f,\emptyset) = PSD^{*}_{1S}(f,\emptyset) + PSD_{XS}(f,\emptyset)} \qquad \text{Eq. 4}$$

where $PSD_{1S}{}^{*}$ is the predicted noise for a single-stream jet with modified fully mixed acoustic Mach number Ma_{mix}* from Eq. 3 and corrected for flight using Equation 2.

The predicted PSD_{1S}* of jet noise using the modified Ma_{mix}* would be a reasonable approximation for internally mixed exhaust systems if the mixer did not create its own, higher frequency noise or if an effective internal acoustic liner were used to remove this source. As mentioned above, the frequency range of this internally generated noise often scales into frequencies at which humans are most sensitive and hence important. We turn now to look at prediction of this 'excess noise', denoted as PSD_{XS} in Eq. 4.

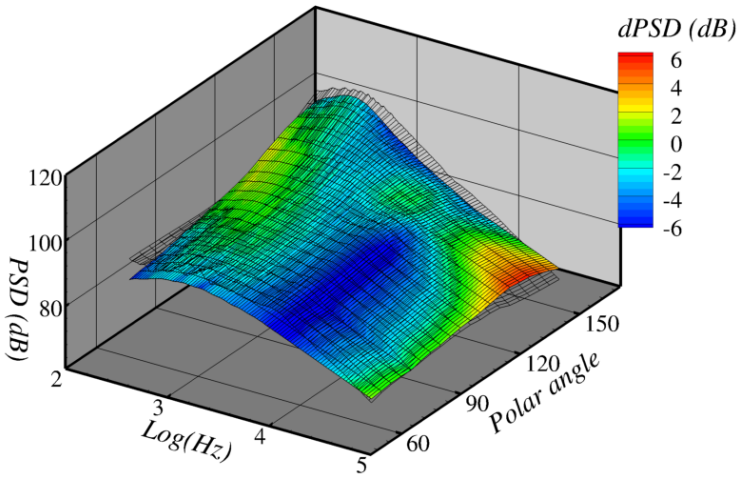

Figure 9 Spectral directivity of internally mixed nozzle with lobed mixer, experiment and single-stream prediction using Ma_{mix}*. Same case as Figure 3.

We continue our model development by subtracting *PSD* of the data from the predicted PSD_{1S}*. Subtraction is done in sound power, not dB, consistent with the idea that the two noise sources are independent. The difference is what we now wish to model as PSD_{XS}.

For nozzles in the historical database, the spectral shape of the extracted PSD_{XS} was striking: roughly a paraboloid in frequency and polar angle. Figure 10 shows the difference between the two mesh surfaces in Figure 9 as a colored surface. The large low-frequency peak at the aft angle is the residual noise imperfectly predicted by PSD_{1S}* and not an independent noise source (see [16] for discussion of using flight effect scaling to separate internal noise sources from external noise sources). What is our focus is the hump at broadside and forward angles and mid frequencies. A superimposed open mesh 'sketch' indicates the hump being discussed.

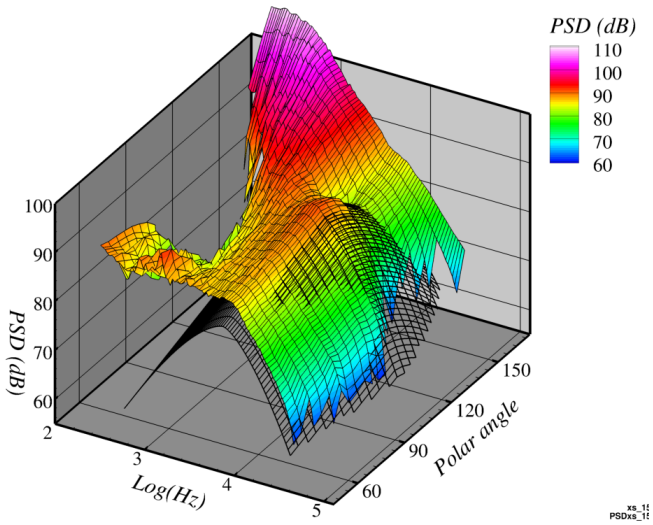

Figure 10 Spectral directivity of excess noise (PSD_{1S}* – Data). Same case as Figure 3.

As discussed in Ref [16], key features of the excess noise are that (i) it is roughly independent of flight speed, (ii) its peak in frequency f_{XS} and peak in polar angle ϕ_{XS} are fixed for a given nozzle geometry over variations in flow conditions. There are variations in ϕ_{XS} and f_{XS} with changes in exhaust system geometries, which will be addressed next.

The variation in peak polar angle ϕ_{XS} between geometries is very slight, being 110° for internal plug nozzles and 120° for external plug nozzles. In the current model we use a fixed value of ϕ_{XS} depending upon whether there is an internal or external plug:

$$\phi_{XS} = \begin{cases} 110°, & if\ internal\ plug \\ 120°, & if\ external\ plug \end{cases} \qquad \text{Eq. 5}$$

The range of peak frequencies observed in experiments was 4.5 - 12kHz for nozzles of roughly the same exit diameter (150mm - 185mm) and inner diameters (250mm). The variation in peak frequency did correlate with distance between the mixers and the nozzle lip, dx_{mix}. For a geometry-based resonance, a convection speed is required; however, both the flow speed from mixer to lip or an acoustic speed from lip back to mixer, will change with flow condition, and yet no such shift with flow condition was discernable in the data. Clearly, an understanding of how the peak frequency of the excess noise is determined still eludes us.

To create a model for the peak frequency which varies with mixing length we simply fit the data, knowing that the model may not hold if the flow is not that of a typical turbofan, such as the models tested here.

$$f_{XS} = 1610/dx_{\text{mix}} \qquad \text{Eq. 6}$$

where dx_{mix}, is distance in meters between mixer and nozzle lips (see Figure 1). Note, dx_{mix}, would typically be roughly 1-2 nozzle diameters in most exhaust systems.

To construct the amplitude model for the excess noise source we calculate the sound power of the 'excess noise' using a band-limited sound power level P_{XS}. The analysis is similar to what was done for the measure P_{1S} but the frequency range used for this metric is higher: $0.67 < f/f_{XS} < 1.5$.

$$P_{XS} = \int_{\frac{f}{f_{XS}}=0.67}^{1.5} \int_{\emptyset} \left(PSD(f,\emptyset) - PSD^{*}_{1S}(f,\emptyset) \right) d\emptyset dSt$$

Looking at the power of this source extracted from data as a function of Ma_{mix}* and NTR_{mix} in Figure 11 we see a wide range of amplitudes. Even for a given value of geometric parameter there is a wide range of amplitudes. In attempting to model this amplitude with the geometric and flow parameters available, we assume independent dependencies on parameters and remove trends one by one, building our model one parameter at a time. The first trend to remove is, unsurprisingly, overall scaling with jet velocity, here represented by Ma_{mix}*. While actual velocities inside the nozzle around the mixer might be more precise, the choice of fully mixed velocity was made with an eye towards simplifying the modeling: Ma_{mix}* is a known quantity while the velocities inside the mixer are not typically known during conceptual design. A surface proportional to $80log_{10}(Ma_{\text{mix}}*)$ is shown with the P_{XS} data in Figure 12. Due to the small range of Ma_{mix}* the value of of the exponent is not very precise but a power of 8 fit slightly better for this extended range of cases than a lower value. No consideration is made for dependence on flight speed M_∞ as there is little dependence on this (as shown in the figure), nor for temperature ratio (not shown here). The lack of dependence on flight speed is expected if the noise source mechanism is associated with flow inside the nozzle or at least near the jet centerline. The lack of temperature ratio dependence may be due to the correlation between Ma_{mix}* and NTR_{mix} in the dataset.

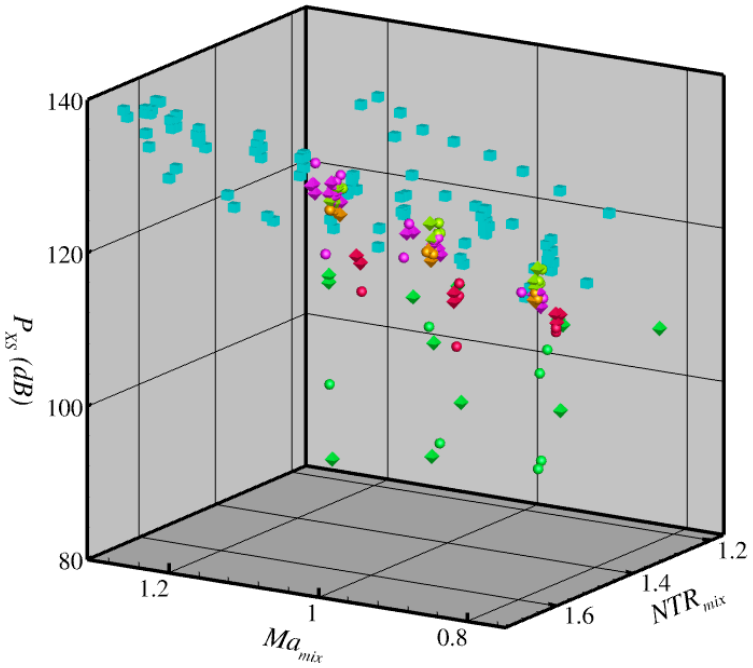

Figure 11 Scatter plot of P_{XS} as a function of mixed acoustic Mach number Ma_{mix}* and NTR_{mix} for all cases in database.

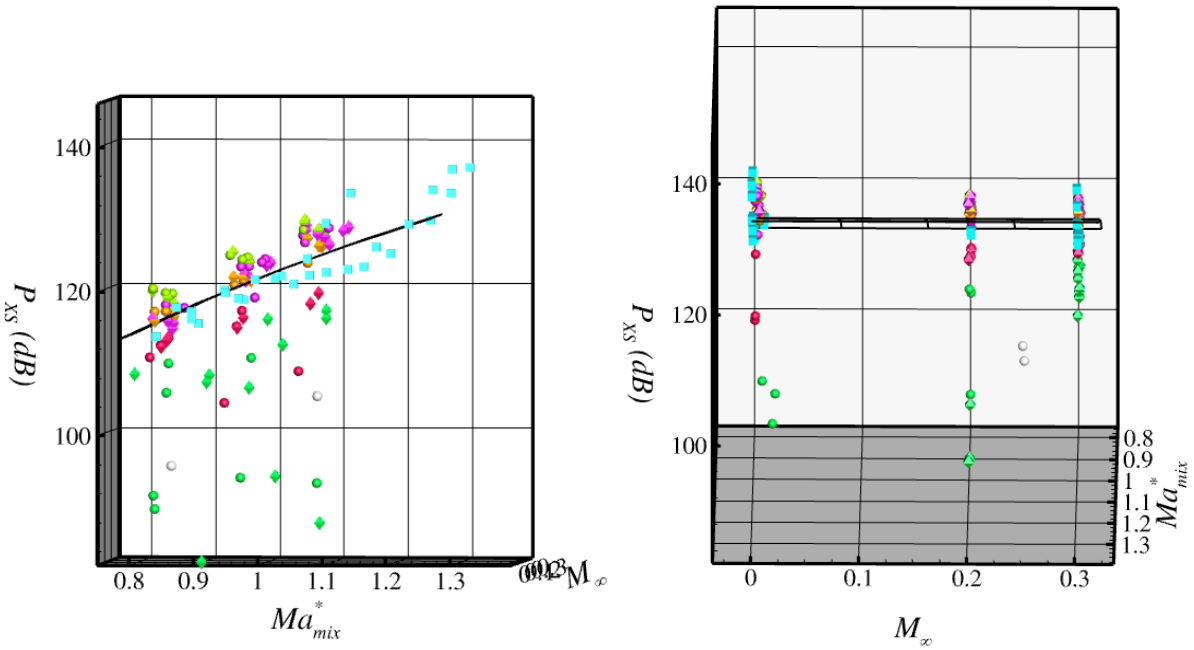

Figure 12 Scatter plot of P_{XS} as a function of mixed acoustic Mach number Ma_{mix} and M_∞ for all cases in database. Mesh surface is $125+80log_{10}(Ma_{mix}^*)$.

The impact of parameters associated with the internal shear layer and the mixer geometry are next to be examined. Figure 13 shows $\Delta P_{XS} = 125+80log_{10}(Ma_{mix}^*) - P_{XS}$, which is P_{XS} after the dependence on $(Ma_{mix}^*)^8$ has been factored out. Looking at ΔP_{XS} projected onto parameters describing lobe divergence h_m/l_m and velocity ratio U_b/U_c, clearly lobe divergence is a significant factor. The amplitude of ΔP_{XS} dramatically decreases with lobe divergence for values of lobe divergence over 0.65, reaching a level that slightly increases with increased lobe divergence. Since ΔP_{XS} is a negative measure of how strong the internal noise source was in the data, the dip in ΔP_{XS} with increasing h_m/l_m roughly correlates the amount of excess noise with the amount of divergence in the mixer lobes . Based on this dataset, it seems mixers with lobe divergence under 0.6 have little excess noise, while those with divergence greater than 0.65 have strong internal noise. The large spread in the amplitude of the extracted ΔP_{XS} for low values of h_m/l_m indicates how sensitive the noise is to this parameter. We will return to this point in the discussion below.

Surprisingly, there is no clear trend with velocity ratio U_b/U_c; one mixer design has ΔP_{XS} increasing with U_b/U_c while another has it decreasing. A simple bilinear dependence on lobe divergence, with a minima at $h_m/l_m = 0.65$, independent of U_b/U_c, is envisioned for this dependence and shown as a gridded surface in Figure 13.

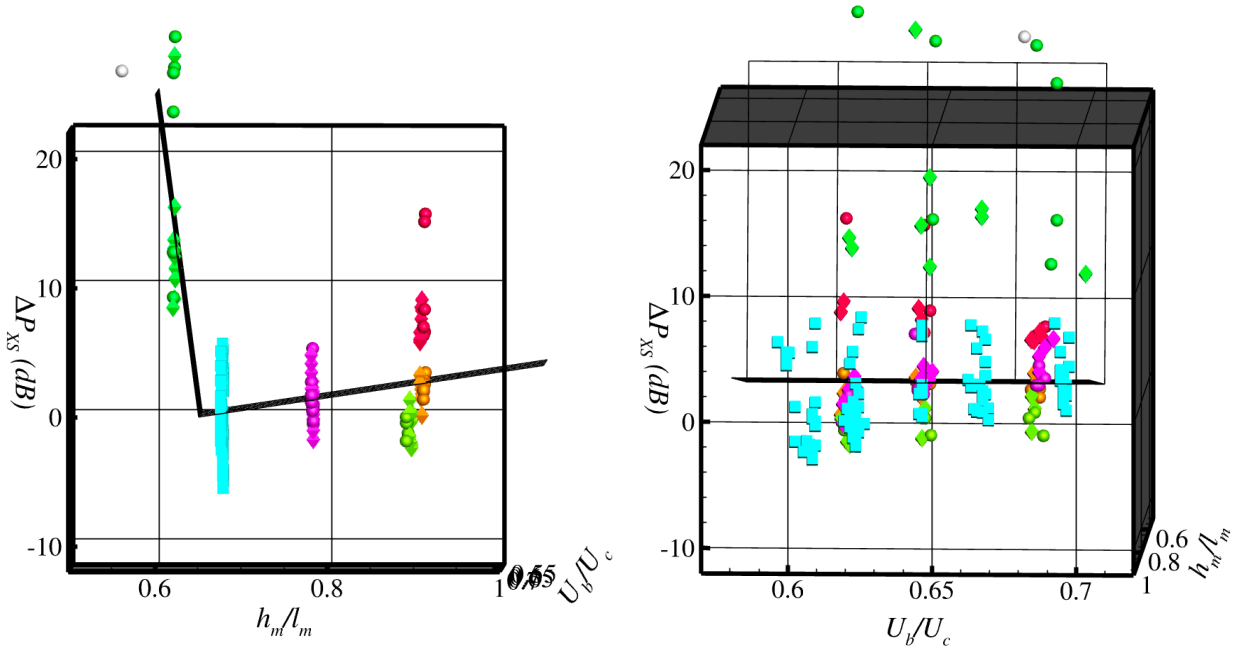

Figure 13 Scatter plot of 80*log*(Ma_{mix}*) - P_{XS} (removing Ma_{mix}* dependence from P_{XS}) as a function of mixer divergence h_m/l_m and velocity ratio U_b/U_c for all cases in database. Mesh surface is model contained in Eq. 8.

One last factor on the amplitude of the excess noise: for nozzles with an external plug there was, on average, a 6dB increase in the amplitude of PSD_{XS} over when an internal plug was used for the same mixer. The external length of the plug did not make much impact, which is in keeping with the phenomena being associated with flow inside the nozzle.

As for the spectral directivity shape, a paraboloid model for this PSD_{XS} is shown in Figure 14. The shape adopted for PSD_{XS}, expressed in dB, was

$$\Omega(f,\phi) = 10log_{10}\left(e^{-\left[\left|log_{10}\left(\frac{f}{f_{XS}}\right)/w_f\right|^{1.5}+|(\phi-\phi_{XS})/w_\phi|^{n_\phi}\right]}\right) \qquad \text{Eq. 7}$$

$$w_f = \begin{cases}0.35, & f < f_{XS}\\ 0.25, & f \geq f_{XS}\end{cases} \qquad w_\phi = \begin{cases}35, & \phi < \phi_{XS}\\ 20, & \phi \geq \phi_{XS}\end{cases} \qquad n_\phi = \begin{cases}1.0, & \phi < \phi_{XS}\\ 1.5, & \phi \geq \phi_{XS}\end{cases}$$

and ϕ_{XS}, f_{XS} are given by Eqs. 5, 6 respectively.

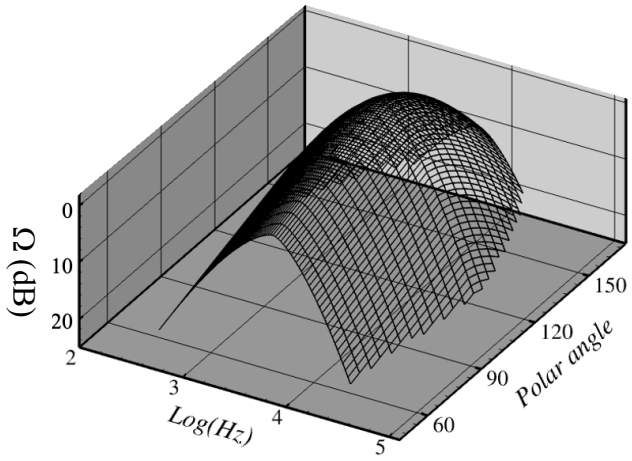

Figure 14 Model for spectral directivity of excess noise $\Omega(f,\phi)$. Also shown in Figure 10.

Combining the amplitude model with the shape model $\Omega(f,\phi)$ from Eq. 6 completes the model for PSD_{XS} expressed in dB:

$$PSD_{XS}(f,\emptyset) = \left[80log_{10}\left(Ma^{*}_{\text{mix}}\right) - \alpha\left(h_m/l_m - 0.65\right) + 6\mathcal{H} + 87\right]\Omega(f,\emptyset) \qquad \text{Eq. 8}$$

$$\alpha = \begin{cases} -500, & h_m/l_m < 0.65 \\ 10, & h_m/l_m \geq 0.65 \end{cases} \qquad \mathcal{H} = \begin{cases} 0, & if\ internal\ plug \\ 1, & if\ external\ plug \end{cases}$$

We can now calculate the P_{XS} from the model in Equation 6 and from data, and compare the error ΔP_{XS} of the model as shown in Figure 15.

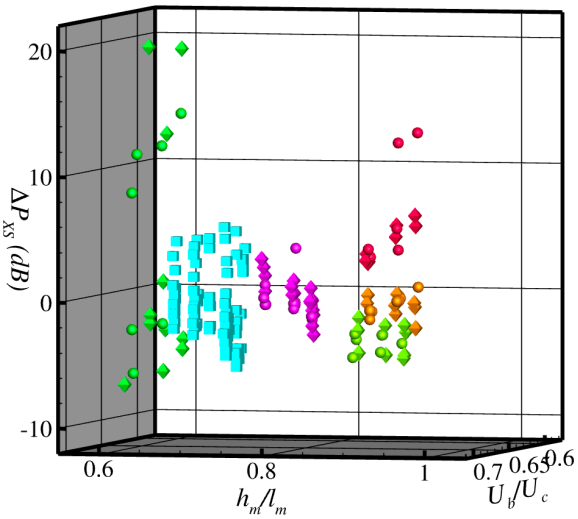

Figure 15 Scatter plot of ΔP_{XS} as a function of mixer lobe height h_m/l_m and Ma_{mix}* for all cases in database.

The dependence of P_{XS} on other flow parameters, such as *BPR* or turbulent convection velocity inside the nozzle, was also examined. However, the dataset available only has a range of *BPR* from 4.5 to 8 and no appreciable dependence was found. We anticipate a dependence on *BPR* as a large sweep of *BPR* from 0 to ∞ would include the cases of single-stream jets at both extremes where there is no excess noise. Until we have a better understanding of the source mechanism behind PSD_{XS} we will not be able to resolve why several mixers of similar lobe divergence have very different internal noise as seen in the vertical spread of points in Figure 15. For the original mission

of providing an empirical model for system-level studies, it is probably best to simply create a model that captures an average of the acoustic performance and use the deviation of the model as a measure of its uncertainty.

To summarize the expected accuracy of the proposed approach, the prediction models PSD_{1S}, PSD_{1S}*, and $PSD_{2S} = PSD_{1S}* + PSD_{XS}$ were used to predict the spectral directivity of all the cases in the database. The experimental and predicted spectral directivities were then scaled to a representative supersonic airliner and flown on a simplified trajectory mimicking takeoff (level flight at M_∞ = 0.3, 1500-ft altitude). Their EPNL values were compared and the differences between the prediction model results and data were compiled as ΔEPNL. The offset and standard deviation of this population of ΔEPNL is given in Table 1, quantifying the expected accuracies of the methods. Interestingly, the standard deviation increased when the adjustment on fully mixed *Ma* was used (going from PSD_{1S} to PSD_{1S}*), but improved quite a bit in both precision and accuracy once the excess noise model was added (PSD_{2S}).

Table 1 Statistics of discrepancies between EPNL calculated from data and from prediction method at different steps of approximation.

ΔEPNL	PSD_{1S}	PSD_{1S}*	PSD_{2S}
Mean	-3.40	-2.09	-0.04
Std dev	2.48	3.33	1.76

Looking forward, the PSD_{2S} model might be improved if the true source (or sources) of the excess noise PSD_{XS} could be established. Currently, physics-based simulations and physical experiments are being pursued to understand the noise mechanism, but it remains an open problem. From analysis of the experimental data and simulations it appears that unsteady separation on the mixer lobes due to the strong divergence angle may be the key source. The abrupt onset of the noise as lobe divergence exceeds 0.65 is one such indication. Acoustic modes within the nozzle probably play into the mechanism. The locking of frequency and directivity with geometry, independent of the flow, point to a mechanism, like duct modes in the nozzle, to trigger the separation and create near-resonant conditions.

There is an additional noise component that should be added to the model for it to fully capture the noise of high-speed propulsion: broadband shock noise. In the case of an internal plug system, the broadband shock will become critical for nozzle pressure ratios (*NPR*) above 1.9. Models for broadband shock noise from round nozzles are available (*e.g.* reference [23]) and should be added to the predicted total jet noise, presumably using the fully mixed NPR and NTR. For systems with an external plug, the acceleration of the flow over the crown of the plug at the nozzle exit produces a single shock at much lower NPR. The noise of the turbulent shear layer interacting with this shock has not been reported, and may need to be separated from the internal 'excess noise' component which was studied here primarily using internal plug geometries.

VI. Summary

Internally mixed exhaust systems have not been in the forefront of engine development since aircraft engines commonly surpassed bypass ratios of 5 or more. As such there are not many publicly available noise prediction methods available for those making system-level studies of propulsion systems for commercial supersonic aviation, where future aircraft are likely to require relatively low bypass-ratio engines but still achieve noise levels comparable to the current fleet. Studies of this kind require a fast prediction of noise with low-fidelity input regarding the flows

and nozzle geometry. They also require a solid basis for their uncertainty assessment. This paper presents a relatively simple noise prediction method for internally mixed exhaust systems and an assessment of its accuracy based on a fairly extensive experimental database. The physical basis for the method is described, with references to research, both historical and ongoing, that were used to create it. Several areas have been identified where understanding is incomplete and further work is needed to reduce the uncertainty of the method. However, this method should allow the prediction of aircraft noise levels and a bound on how much worse or better it might be as the nozzle design becomes more detailed.

Acknowledgements

This work was performed under NASA's Commercial Supersonic Technology Project. The support of the Project is gratefully acknowledged. The large eddy simulations of Gerrit Stich and the duct resonance simulations of David Stephens boosted confidence that the unique spectral directivity of the excess noise was likely due to interaction of unsteady separation on the lobes and the nozzle duct acoustic modes, guiding the modeling effort. The author also thanks Greg Busch for his review of the manuscript.

References

[1] Banks, W. V., "Advanced Parametric Lobe Mixer Concepts for Internally Mixed Nozzles," *AIAA AVIATION 2023 Forum*, American Institute of Aeronautics and Astronautics. https://doi.org/10.2514/6.2023-3469

[2] Banks, W. V., "Optimization of a Parametric Lobe Mixer for Internally Mixed Nozzles," *AIAA AVIATION 2022 Forum*, American Institute of Aeronautics and Astronautics. https://doi.org/10.2514/6.2022-3261

[3] Goodykoontz, J. H., "Experiments on High Bypass Internal Mixer Nozzle Jet Noise," *NASA-TM-83020*, NASA, 1982.

[4] Kozlowski, H., and Kraft, G., "Experimental Evaluation of Exhaust Mixers for an Energy Efficient Engine," *16th Joint Propulsion Conference*, American Institute of Aeronautics and Astronautics, 1980. https://doi.org/10.2514/6.1980-1088

[5] Wright, C., Blaisdell, G., and Lyrintzis, A., "The Effects of Various Mixer Shapes on Jet Noise," *9th AIAA/CEAS Aeroacoustics Conference and Exhibit*, American Institute of Aeronautics and Astronautics, 2003. https://doi.org/10.2514/6.2003-3251

[6] Mengle, V. G., and Dalton, W. N., "Lobed Mixer Design for Noise Suppression Vol 1," *NASA/CR—2002-210823/VOL1*, 2002.

[7] Mengle, V. G., and Dalton, W. N., "Lobed Mixer Design for Noise Suppression Vol2," *NASA/CR--2002-210823/VOL2*, 2002.

[8] Mengle, V., "Anomalous Effect of Nozzle Length Reduction on Jet Noise of Forced Mixers," *5th AIAA/CEAS Aeroacoustics Conference and Exhibit*, American Institute of Aeronautics and Astronautics, 1999. https://doi.org/10.2514/6.1999-1968

[9] Garrison, L., Lyrintzis, A., Blaisdell, G., and Dalton, W., "Computational Fluid Dynamics Analysis of Jets with Internal Forced Mixers," *11th AIAA/CEAS Aeroacoustics Conference*, American Institute of Aeronautics and Astronautics, 2005. https://doi.org/10.2514/6.2005-2887

[10] Krejsa, E., and Saiyed, N., "Characteristics of Residual Mixing Noise from Internal Fan/Core Mixers," *35th Aerospace Sciences Meeting and Exhibit*, American Institute of Aeronautics and Astronautics, 1997. https://doi.org/10.2514/6.1997-382

[11] Tester, B., and Fisher, M., "A Contribution to the Understanding and Prediction of Jet Noise Generation by Forced Mixers: Part III Applications," *12th AIAA/CEAS Aeroacoustics Conference (27th AIAA Aeroacoustics Conference)*, American Institute of Aeronautics and Astronautics, 2006. https://doi.org/10.2514/6.2006-2542

[12] Garrison, L., Lyrintzis, A., and Blaisdell, G., "RANS-Based Noise Predictions of Jets with Internal Forced Mixers," *12th AIAA/CEAS Aeroacoustics Conference (27th AIAA Aeroacoustics Conference)*, American Institute of Aeronautics and Astronautics, 2006. https://doi.org/10.2514/6.2006-2599

[13] Ramsey, D. N., Gavin, J., and Ahuja, K. K., "Howling in a Model-Scale Nozzle Related to Shock-Induced Boundary-Layer Separation at the Nozzle Exit," presented at the 2023 AIAA Aviation Forum, San Diego, CA,U.S.A., 2023.

[14] Ramsey, D. N., Mayo, R., and Ahuja, K. K., "Howling in a Model-Scale Internally Mixed Confluent Nozzle Related to Excited Core-Jet Instability," presented at the 2023 AIAA Aviation Forum, San Diego, CA,U.S.A., 2023.

[15] Wojno, J., Martens, S., Bridges, J., and Brown, C., "Acoustic and Flow-Field Measurements of a Long Duct Chevron Mixer," *13th AIAA/CEAS Aeroacoustics Conference (28th AIAA Aeroacoustics Conference)*, American Institute of Aeronautics and Astronautics, 2007. https://doi.org/10.2514/6.2007-3600

[16] Bridges, J., "Diagnosing Noise Features of Internally Mixed, External Plug Exhaust Systems," *2023 AIAA Aviation Forum*, American Institute of Aeronautics and Astronautics, San Diego,CA,U.S.A., 2023.

[17] Bridges, J. E., and Wernet, M. P., "Noise of Internally Mixed Exhaust Systems With External Plug For Supersonic Transport Applications," presented at the AIAA AVIATION 2021 FORUM, VIRTUAL EVENT, 2021. https://doi.org/10.2514/6.2021-2218

[18] Bridges, J., Wernet, M. P., and Podboy, G. G., "Plug20 Test Report," NASA Technical Memo NASA/TM—2021-10291, March 2021.

[19] Ahuja, K. K., Tester, B., and Tanna, H. K., "The Free Jet as a Simulator of Forward Velocity Effects on Jet Noise," NASA/CR—1978-3056, October 1978.

[20] Khavaran, A., and Bridges, J., "Development of Jet Noise Power Spectral Laws Using SHJAR Data," *15th AIAA/CEAS Aeroacoustics Conference (30th AIAA Aeroacoustics Conference)*, American Institute of Aeronautics and Astronautics, 2009. https://doi.org/10.2514/6.2009-3378

[21] Viswanathan, K., "Scaling Laws and a Method for Identifying Components of Jet Noise," *AIAA Journal*, Vol. 44, No. 10, 2006, pp. 2274–2285. https://doi.org/10.2514/1.18486

[22] Viswanathan, K., and Czech, M. J., "Measurement and Modeling of Effect of Forward Flight on Jet Noise," *AIAA Journal*, Vol. 49, No. 1, 2011, pp. 216–234. https://doi.org/10.2514/1.J050719

[23] Tam, C. K. W., "Broadband Shock Associated Noise from Supersonic Jets Measured by a Ground Observer," *AIAA Journal*, Vol. 30, No. 10, 1992, pp. 2395–2401. https://doi.org/10.2514/3.11239